

IEEE

GEOSCIENCE AND REMOTE SENSING LETTERS

A PUBLICATION OF THE IEEE GEOSCIENCE AND REMOTE SENSING SOCIETY



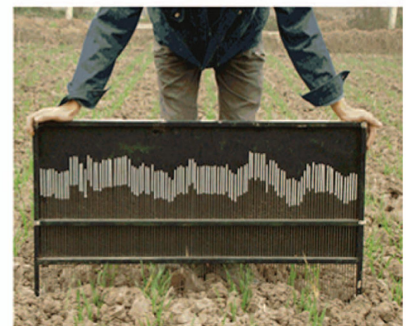
JUNE 2016

VOLUME 13

NUMBER 6

IGRSBY

(ISSN 1545-598X)



Photographs of wheat field growth cycle.

IEEE

GEOSCIENCE AND REMOTE SENSING LETTERS

A PUBLICATION OF THE IEEE GEOSCIENCE AND REMOTE SENSING SOCIETY



JUNE 2016

VOLUME 13

NUMBER 6

IGRSBY

(ISSN 1545-598X)

PAPERS

Atmosphere

- Fade-Slope Model for Rain Attenuation Prediction in Tropical Region *D. Das and A. Maitra* 777
Ionospheric Spatial Gradient Detector Based on GLRT Using GNSS Observations *S. Raghunath and D. V. Ratnam* 875

Oceans and Water

- Standard and Regional Bio-Optical Algorithms for Chlorophyll *a* Estimates in the Atlantic off the Southwestern Iberian Peninsula
. *S. Cristina, D. D'Alimonte, P. C. Goela, T. Kajiyama, J. Icely, G. Moore, B. Fragoso, and A. Newton* 757
Object-Based Arctic Sea Ice Ridge Detection From High-Spatial-Resolution Imagery
. *X. Miao, H. Xie, S. F. Ackley, and S. Zheng* 787
Retrieval of Wind Stress at the Ocean Surface From AltiKa Measurements
. *M. M. Ali, M. A. Bourassa, S. A. Bhowmick, R. Sharma, and K. Niharika* 821

Vegetation and Land Surface

- Influence of Row Wheat on Radar Backscatter for Azimuthal Look Angles at L-, S-, C-, and X-Bands
. *L. He, L. Tong, J. Shi, Y. Chen, Y. Li, C. Guo, and B. Wu* 811
Leaf Area Index Inversion of Winter Wheat Using Modified Water-Cloud Model
. *L. Tao, J. Li, J. Jiang, and X. Chen* 816
Polarimetric Decomposition for Monitoring Crop Growth Status
. *H. Wang, R. Magagi, and K. Goita* 870

Surface and Subsurface Properties

- A Phase-Gradient-Autofocus Algorithm for the Recovery of MARSIS Subsurface Data
. *M. Restano, R. Seu, and G. Picardi* 806

Image Processing, Analysis, and Classification

- Bag-of-Visual-Words Scene Classifier With Local and Global Features for High Spatial Resolution Remote Sensing Imagery
. *Q. Zhu, Y. Zhong, B. Zhao, G.-S. Xia, and L. Zhang* 747
Bundle Block Adjustment of Tilt-Shift-Based Multidigital Camera System by Rigorous Orientation Model
. *T. Sun, J.-Y. Fang, and Y. Li* 836
Developing an Index for Detection and Identification of Disease Stages
. *D. Ashourloo, A. A. Matkan, A. Huete, H. Aghighi, and M. R. Mobasheri* 851

(Contents Continued on Page 746)



Feature Extraction for Patch-Based Classification of Multispectral Earth Observation Images	<i>F.-A. Georgescu, C. Vaduva, D. Raducanu, and M. Datcu</i>	865
DEM-Aided Bundle Adjustment With Multisource Satellite Imagery: ZY-3 and GF-1 in Large Areas	<i>M. Zheng and Y. Zhang</i>	880
Hyperspectral Data Processing		
A Fast Spatial–Spectral Preprocessing Module for Hyperspectral Endmember Extraction.	<i>F. Kowkabi, H. Ghassemian, and A. Keshavarz</i>	782
Spectral Variation Alleviation by Low-Rank Matrix Approximation for Hyperspectral Image Analysis	<i>S. Mei, Q. Bi, J. Ji, J. Hou, and Q. Du</i>	796
Radar Systems		
Improved Phase-Encoding Calibration for Active Phased-Array Antennas of SAR	<i>Y. Gong, R. Wang, and P. Wang</i>	767
Compensation for High-Frequency Vibration of Platform in SAR Imaging Based on Adaptive Chirplet Decomposition	<i>Y. Wang, Z. Wang, B. Zhao, and L. Xu</i>	792
An Inverse Extended Omega-K Algorithm for SAR Raw Data Simulation With Trajectory Deviations	<i>Y. Huai, Y. Liang, J. Ding, M. Xing, L. Zeng, and Z. Li</i>	826
MT-BCS-Based Two-Dimensional Diffraction Tomographic GPR Imaging Algorithm With Multiview–Multistatic Configuration	<i>Y. Sun, L. Qu, S. Zhang, and Y. Yin</i>	831
Angular Superresolution for Scanning Radar With Improved Regularized Iterative Adaptive Approach.	<i>Y. Zhang, Y. Zhang, Y. Huang, W. Li, and J. Yang</i>	846
Synthetic Aperture Radar		
Structure Filling and Matching for Three-Dimensional Reconstruction of Buildings From Single High-Resolution SAR Image	<i>D. Feng and W. Chen</i>	752
FOPEN Target Detection via Joint Space/Angle Variation	<i>M. A. Sletten and J. Brozana</i>	762
On the Importance of Multireference Points for CKF Phase Unwrapping in Areas With Discontinuous Quality Maps.	<i>W. Liu, Z. Bian, Q. Zhang, Z. Liu, and S. Lei</i>	772
Detecting Cars in VHR SAR Images via Semantic CFAR Algorithm	<i>Y. Huang and F. Liu</i>	801
DLSLA 3-D SAR Imaging Based on Reweighted Gridless Sparse Recovery Method	<i>Q. Bao, X. Peng, Z. Wang, Y. Lin, and W. Hong</i>	841
SAR Image Change Detection Based on Multiple Kernel K-Means Clustering With Local-Neighborhood Information.	<i>L. Jia, M. Li, P. Zhang, Y. Wu, and H. Zhu</i>	856
Comparing Compact and Quadrature Polarimetric SAR Performance	<i>R. K. Raney</i>	861
